TAO, Vol.7, No.1, 31-42, March 1996

A Study of the Characteristics of Scattering Attenuation by Physical Modelling

CHAO-HUI HSIEH[1] and YOUNG-FO CHANG[1]

(Manuscript received 20 February 1995, in final form 21 December 1995)

ABSTRACT

Scattering attenuation $(1/Q_s)$ depends not only on wave frequency but also on scatterer size. Using void holes as scatterers in a thin duralumin plate, and with the ka value (k is the wave number, a the scatterer radius) being changed systematically from 0.05 to 5, the fluctuation of direct waves between a homogeneous and a scattering medium are observed in order to calculate the scattering attenuation by 2-D physical model experiments. The experimental results show that $1/Q_s$ has a peak around ka = 0.5. At high frequency, $1/Q_s$ is proportional to $(ka)^{-1}$, whereas at low frequency the decay of $1/Q_s$ relative to $(ka)^4$ is steeper than predicted by Rayleigh scattering. The medium can be considered to be a quasi-homogeneous one, and the scattering effect can be neglected when ka < 0.05. The velocity fluctuation has a sharp change at ka = 0.5. The velocity of the scattering medium doesn't change when 0.5 < ka, is less than that in a homogeneous medium and exhibits a constant fluctuation when ka < 0.5. Whether the wave length is smaller or greater than the scatterer size, the P- and S-waves have the same scattering attenuation coefficients if they have the same ka value.

(Key words: Scattering attenuation, Intrinsic attenuation, Physical model)

1. INTRODUCTION

Absorption of seismic energy while propagating in a medium is a result of two major factors. The first factor is the intrinsic attenuation $(1/Q_i)$ due to the transfer of seismic energy to heat caused by friction. The second factor is the result of scattering attenuation $(1/Q_s)$ whereby seismic waves are scattered by the heterogeneity of the media. In this case, the scattered energy isn't absorbed but merely redistributed in space and time. The intrinsic attenuation is less complicated than the scattering attenuation because the latter depends not only on the frequency but also on the scatterer size. Nevertheless, field surveys often involve some kind of combination effect of these two factors (Frankel, 1991; Mayeda *et al.*, 1991;

[1] Institute of Geophysics, National Central University, Chung-Li, Taiwan, R.O.C.

Fehler, *et al.*, 1992; Castro and Munguia, 1993) since it is difficult to separate one from the other.

Under Rayleigh scattering, when $ka << 1$, (where k is the wave number and a is the scatterer radius), $1/Q_s$ can be approximated by f^{-1}(f is frequency), where n is the dimensional factor (n = 1 for 1-D, n = 2 for 2-D and n = 3 for 3-D). However, when $1<< ka$, the $1/Q_s$ can be relative to f, and attained its peak for the moderate ka values (Menke, 1984; Menke, *et al.*, 1985). Sato (1984) used statistical methods and Born approximation to estimate the scattering Q_s and showed that the maximum $1/Q_s$ occurs at ka' = 3.2 (a' is the inhomogeneity correlation distance) for the P-wave and at ka' = 1.9 for S-wave. For Rayleigh scattering, the $1/Q_s$ values of both the P- and S-waves were proportional to the f^3 for low and intermediate frequencies, but they were the reciprocal of the frequency at high frequencies. Using a finite-difference scheme, Frankel and Claton (1986) computed the all wave field and measured $1/Q_s$ directly from the synthetic seismograms. They found that the relationship between $1/Q_s$ and ka' depended on the scatterer's random model and that a peak value of $1/Q_s$ existed around ka' =1$\sim$2. Benites *et al.* (1992), using the boundary integral method, simulated the synthetic seismograms of scattered SH waves from cavities in the 2-D homogeneous elastic media. They concluded that $1/Q_s$ increased rapidly with ka, reaching its peak at around ka = 1 and falling with ka > 1.

Kikuchi (1981a, b) studied the scattering effects of P-, S- and SH waves caused by cracks which are a great contrast to the surrounding medium. He found that $1/Q_s$ had the peak value at ka'' =1$\sim$2 (a'' is one half of the crack length). Yamashita (1990), Kawahara and Yamashita (1992) also studied crack scattering and found that $1/Q_s$ had its peak value at ka'' = 1. At high frequency, $1/Q_s$ was proportional to f^{-1}, but at low frequency, proportional to f^3.

Menke *et al.* (1985) calculated the apparent attenuation of the P- wave in a 3-D aluminum block with a random distribution of parallel cylindrical voids. They found that $1/Q_s$ was proportional to the square of the frequency at low frequency. Matsunami (1991) used a 2-D physical model to study coda Q and found that $1/Q_s$ value had its peak around ka = 1$\sim$1.5, but decreased steeply on both sides of the peak.

The Q value for body waves at low frequency(f < 0.5 Hz) has not been completely observed. Statistically, it is necessary to assume the probability function of scatterers in studying the attenuation in the random model. Due to the limitation of computer capacity, it is also hard to calculate numerically the scattering effects for elastic waves with numerous scatterers in a wide frequency range. As such, it is valuable to survey the variation of the Q values associated with a broad band of ka by 2-D physical modelling. The authors of the present study measure the direct scattered waves under distinct ka's to determine the wave attenuation and also the scattering relationship between Q_s and ka.

2. EXPERIMENT

The setup of the 2-D physical seismic model is shown in Figure 1. The pulse generator triggers the function generator and digital oscilloscope simultaneously every 20 milliseconds. Then the function generator sends a driving wave through a power amplifier to the piezoelectric source-transducer. When this transducer is excited by a driving wave, it emits ultrasonic waves propagating through the medium which are recorded by the piezoelectric receiver-transducer. The recorded signal through the preamplifier and the band-pass filter is stored in a digital oscilloscope and then read via the GPIB interface.

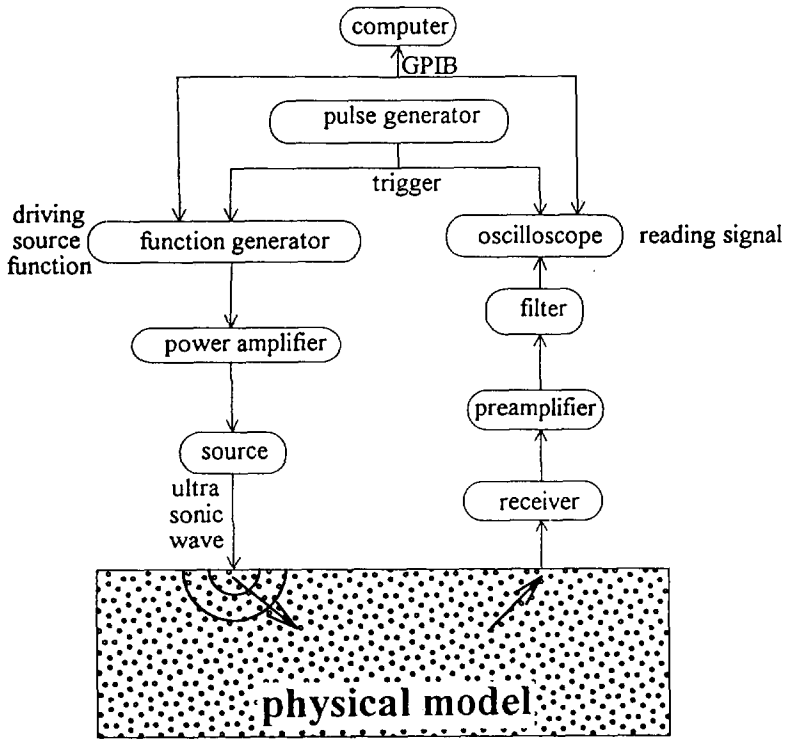

Fig. 1. A block diagram to represent the seismic physical modeling apparatus.

The procedures followed in the experiments are shown in Figure 2. The acquisition parameters, including the sampling rate, record length, filter band, stacking number, stacking rate, source function and amplifier gain are set first. The ultrasonic waves propagate into the model and then interact with the obstacle. The seismic signals detected by the receiver-transducer are digitized, stacked and averaged by the oscilloscope. The personal computer reads and stores the stacked signal. The program stops as this job ends; otherwise, the detector would move to another position and make a new measurement.

The source- and receiver-transducers are made of PZT-4 and PZT-5 ceramics, respectively. The recording amplitude error of the system is about 5%, and travel time error is less than 0.2 microseconds. There exists a simple scaling factor to correlate the laboratory seismic model with the field, as suggested by Pant *et al.* (1988):

$$\frac{L_m}{\lambda_m} = \frac{L_e}{\lambda_e}, \tag{1}$$

where L is the characteristic length, λ is an appropriate wave length and the subscripts m and e represent the 'model' and the 'earth', respectively.

In this experiment, a scale factor of 10^5 is used to correspond to the field case. This means that 1 cm in the model is equivalent to 1 km in the field, 100 KHz in the model equals 1 Hz in the field, and 1 micro second in the model equals 0.1 second in the field.

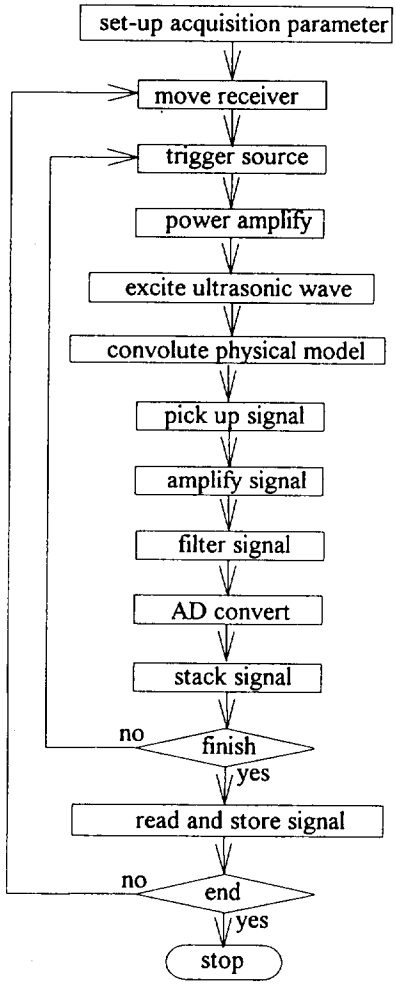

Fig. 2. The flow chart of the procedures followed in the experiment.

3. MODELS

The duralumin plate is used as a homogeneous medium in the laboratory experiment. The length, width and thickness of this plate are 243.6 cm, 122 cm and 0.1 cm, respectively. The holes in the models serve as the scatterers. Two models with different values of scatterer size are used : M1 (1 cm radius) and M2 (0.1 cm radius). The scatterers are randomly distributed over the duralumin plate, and by increasing their number the scattering effect is enhanced. There are three cases with different numbers of scatterers (30, 95 and 188) for model M1. The related values of percentage of the scatterer volume ratio to the plate, S.V.R., are 0.32, 1 and 2 for the three cases. For model M2, there are 2983, 5935 and 11953 scatterers with the S.V.R. values of 0.32, 0.63 and 1.26, respectively. The signals are measured firstly for a homogeneous duralumin plate and then measured again after the holes are made in the plate. Thus, the results for the homogeneous model and the models with the holes are compared in order to calculate the Q_s values.

The dominant frequencies of the input source wavelet are set to be 500 KHz, 200 KHz, 100 KHz and 45 KHz. The model parameters and input signals are shown in Table 1. The ka value changes from 0.05 to 5.9 for P-wave and from 0.1 to 10.1 for S-wave.

Table 1. Model parameters.

Duralumin plate								
Density (g/cm^3)	2.7							
Wave type	P-wave				S-wave			
Attenuation coefficient (1/cm)	$\alpha_p = 0.0029 \pm 0.0004$				$\alpha_s = 0.0046 \pm 0.0018$			
Velocity (m/sec)	Vp=5370				Vs=3100			
Frequency (KHz)	500	200	100	45	500	200	100	45
Wave number (k,1/cm)	5.85	2.34	1.17	0.53	10.1	4.05	2.03	0.91
ka (M1, a=1 cm)	5.9	2.3	1.2	0.5	10.1	4.05	2.0	0.9
ka (M2, a=0.1 cm)	0.59	0.23	0.12	0.05	1.0	0.41	0.2	0.09

The detectors are uniformly placed along two arcs with the source as the center. The distances between the source and each arc are 243.6 cm and 203.6 cm for P-wave but 140 cm and 90 cm for S-wave (see Figure 3). The radial component for P-wave and the transverse component for S-wave are measured at each detector station. Since the maximum wave length of the input signal is about 12 cm, the arc length is set to be 20 cm to cover the range of about two-wave lengths. At each arc profile, 21 traces are recorded and summed together to reduce random noise and local scattering waves. The direct waves in the ensemble seismograms can be treated as the average scattering effect. The energy of the S-wave is much weaker than that of the P-wave and can only be analyzed in a strong scattering condition.

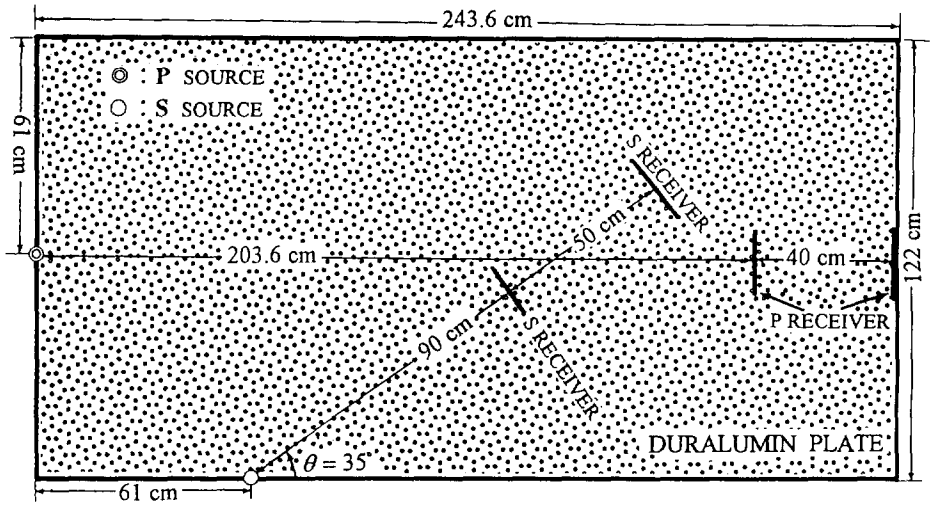

Fig. 3. The schematic diagram of the model used in experiments. The 21 detectors distribute uniformly in a 20 cm arc profile and the source is located at the center.

4. RESULTS

For P-wave propagation, the ensemble trace averaging 21 traces detected on the arc at 243.6 cm from the source is shown in Figures 4 and 5 for models M1 and M2, respectively. From top to bottom in the Figures 4 and 5, the seismograms are shown with different S.V.R.'s. and the amplitude of the scattered waves decreases with an increasing S.V.R. for model M1. However, the scattered amplitude at high frequency (e.g. 500 KHz) for model M2 decays faster than that for M1. Nevertheless, there is no obvious attenuation of the scattered amplitude of model M2 at low frequency (45 KHz).

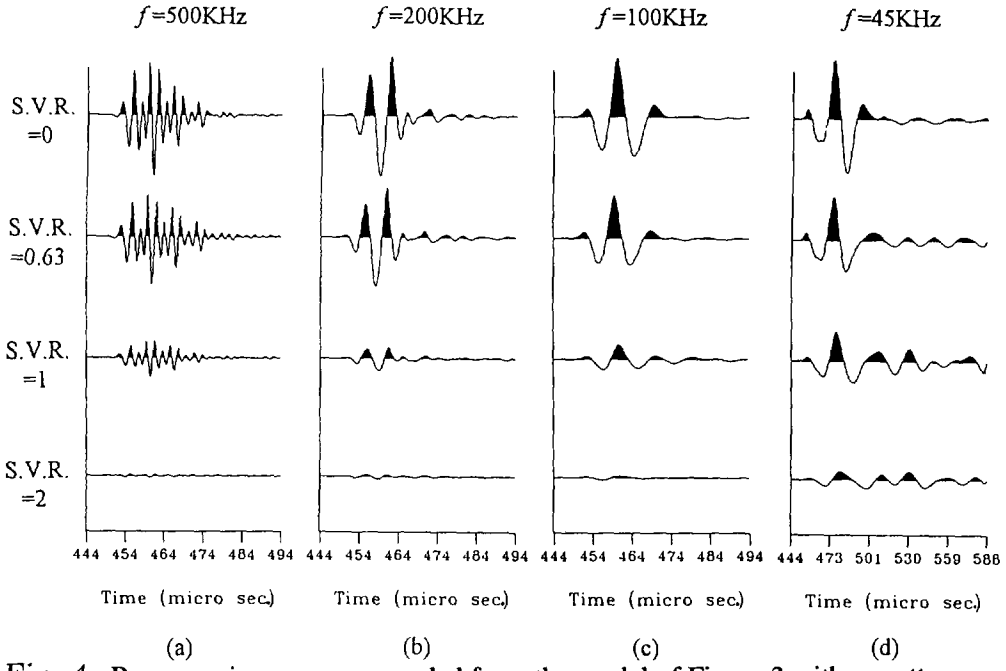

Fig. 4. P-wave seismograms recorded from the model of Figure 3 with a scatterer radius of 1 cm for different values of $S.V.R.$: top traces for $S.V.R.$ = 0, second traces for S.V.R. = 0.32, third traces for $S.V.R.$ = 1 and bottom traces for $S.V.R.$ = 2. The dominant frequency used is 500 KHz for (a), 200 KHz for (b), 100 KHz for (c) and 45 KHz for (d).

For a point source, the far field amplitude is in proportion to $1/\sqrt{d}\rho V_p^2$ where d is the travel distance, ρ is the density, and Vp is the P-wave velocity (Aki and Richards, 1980). Figure 6 shows the relationship of the normalized observed amplitude for the scattering medium versus the normalized theoretical amplitude calculated from $1/\sqrt{d}\rho V_p^2$ with ka = 0.05. The numbers beside the data represent the S.V.R.'s. The straight line in the figure is the theoretical amplitude corresponding to distinct $1/\sqrt{d}\rho V_p^2$ values. The amplitude of the P-wave with different S.V.R.'s in the duralumin plate shown in Figure 6 can be expressed as the P-wave propagating in an another homogeneous medium with distinct elastic parameters.

The velocity of a scattering direct wave for model M2 shown in Figure 5 changes slightly with respect to the SVR values, but it does not seem to change for model M1 (Figure

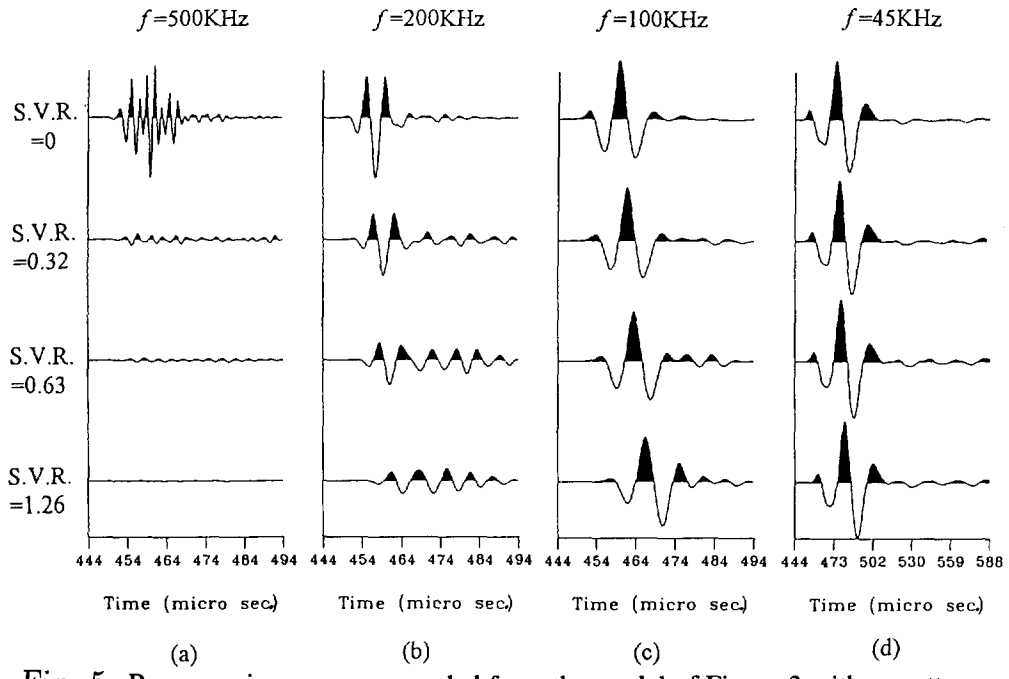

Fig. 5. P-wave seismograms recorded from the model of Figure 3 with a scatterer radius of 0.1 cm for different values of $S.V.R.$: top traces for $S.V.R.$ = 0, second traces for $S.V.R.$ = 0.32, third traces for $S.V.R.$ = 0.63 and bottom traces for $S.V.R.$ = 1.26. The dominant frequency used is 500 KHz for (a), 200 KHz for (b), 100 KHz for (c) and 45 KHz for (d).

4). The greater the scattering effect, the slower the velocity of the scattering direct wave is. The velocity fluctuations of P- and S-waves for ka are shown in Figure 7 where a sharp change at ka = 0.5 is noted.

In this study, the Q_s is calculated by using the spectrum ratio method. The amplitude $A_h(d, f)$ in a homogeneous plate received at a distance d from the source can be expressed as :

$$A_h(d, f) = S(f) \cdot A_s(f) \frac{e^{-\alpha(f,a)\cdot d}}{\sqrt{d}}, \tag{2}$$

where $S(f)$ is the system response, $A_s(f)$ is the source function, and $\alpha(f, a)$ is the intrinsic attenuation coefficient. The variation of the intrinsic attenuation coefficient can be neglected because the coefficient itself is very small, although a small volume change does actually exist. The amplitude of the scattering waves $A(d, f)$ at a distance d can be expressed as :

$$A(d, f) = S(f) \cdot A_s(f) \frac{e^{-\alpha(f,a)\cdot d}}{\sqrt{d}}, \tag{3}$$

where $g(f, a)$ is the scattering coefficient. Equation (3) is divided by (2) and logarithm is taken on both sides :

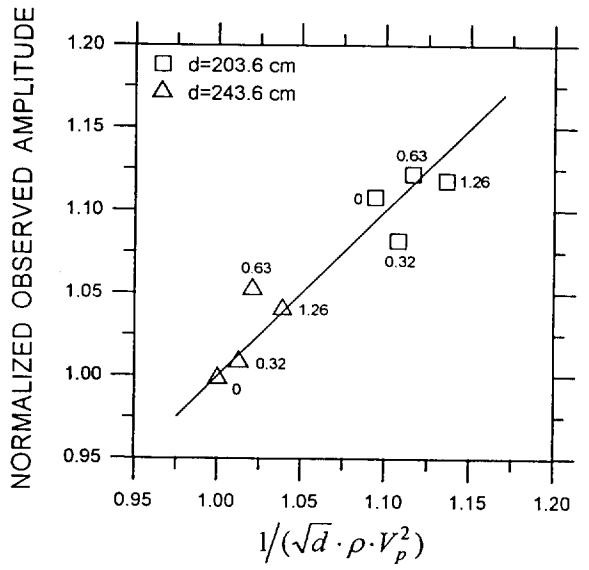

Fig. 6. The relationship between the normalized observed amplitude (Y-axis) and normalized theoretical amplitude calculated from $1/\sqrt{d}\rho V_p^2$ for a P-wave with a ka = 0.05. The numbers beside the data represent the S.V.R. values.

$$\log\left(\frac{A(d,f)}{A_h(d,f)}\right) = -g(f,a)\cdot d. \tag{4}$$

Then, the $Q_s(f,a)$ can be expressed as:

$$Q_s(f,a) = \frac{\phi f}{g(f,a)V}, \tag{5}$$

where V is the P- or S- wave velocity.

After truncating the direct waves from the ensemble seismograms, the Fourier amplitude spectrum is calculated. For the homogeneous medium, the frequency of the peak Fourier amplitude is taken as the dominant one. Thus, the average of the amplitude spectra whose amplitudes are greater than 90% of the peak Fourier amplitude at the dominant frequency is taken. For the scattering Fourier amplitude spectrum, the amplitudes are averaged over the frequency range which is the same as that in the homogeneous medium. Using Equation (4), the scattering attenuation coefficient can be calculated, as can the $1/Q_s$ by Equation (5). The variation of $1/Q_s$ versus ka is shown in Figure 8.

From the experimental results (Figure 8), the peak value of $1/Q_s$ exists at about ka = 0.5. For 1 < ka, the relationship between $1/Q_s$ and ka for both P- and S-waves can be expressed as $1/Q_s \propto (S.V.R.)\cdot(ka)^{-1}$. For 0.12 < ka < 0.23, the $1/Q_s$ for P- and S-waves is proportional to $(ka)^4$, where the wave lengths are larger than the scatterer size.

The scattering attenuation coefficients of P- and S-waves related to ka are shown in Figure 9. It is obvious that the scattering attenuation coefficients for both P- and S-waves have the same trend. Accordingly, it can be concluded that the scattering attenuation coefficients for both P- and S-waves would be equivalent if they had the same ka values.

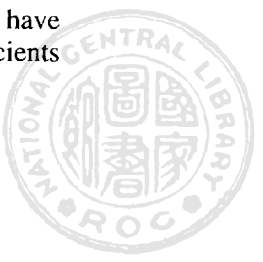

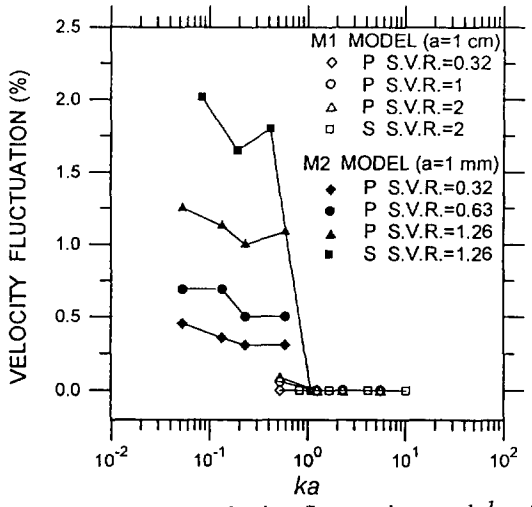

Fig. 7. The relationship between velocity fluctuation and ka for P- and S-waves.

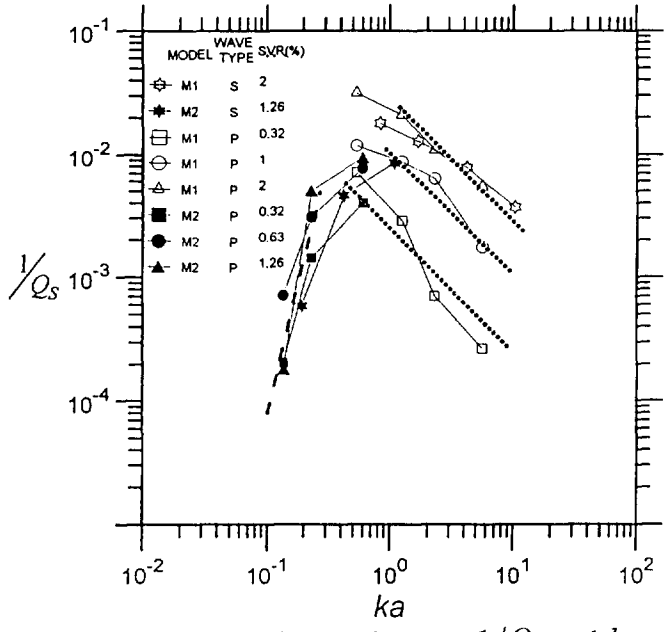

Fig. 8. The relationship between $1/Q_s$ and ka.

5. DISCUSSION

When $ka < 0.01$ and the scattering effect is very weak or nil, the material can be called a quasi-homogeneous medium (Wu and Aki, 1988). Although a void hole with a sharp physical property contrast to the master materials has stronger scattering effects than one with a weak contrast to earth materials, it can still serve as the scatterer in studying scattering attenuation in seismic wave propagation. Figure 6 shows that the scattering effects can be neglected, and the

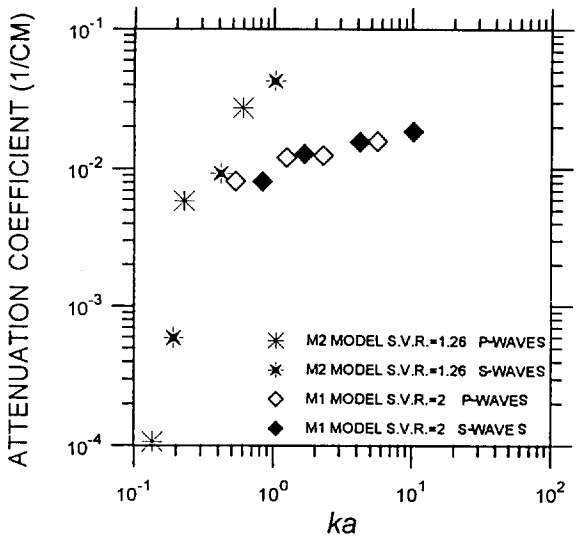

Fig. 9. The relationship between the scattering attenuation coefficient and ka.

medium can be treated as an equivalent homogeneous medium with other elastic parameters when $ka \leq 0.05$.

Menke *et al.* (1985) investigated the attenuation problem and also found that the direct waves arrive later in a heterogeneous medium than in a homogeneous one. Kawahara and Yamashita (1992) calculated the Q_s from the fracture zone and found that the velocity fluctuation changed at $ka'' = 1$. When $ka'' < 1$, the velocity fluctuation remained about constant, whereas the velocity fluctuation decreased with increasing ka'', when $1 < ka''$. The difference in the velocity fluctuation between ka and ka'' can be interpreted as the result of different scatterers, such as cracks and void holes.

At high frequencies, the $1/Q_s$ is proportional to f (Menke, 1984; Sato 1984; Yamashita, 1990; Kawahara and Yamashita, 1992) and is also consistent with the measurements $1/Q_s \propto (S.V.R.)) \cdot (ka)^{-1}$ derived from the present experiment. When the scatterer size is equivalent or larger than the wave lengths, the scattering effect could be expressed by ray theory, and the attenuation due to scattering loss was independent of frequency (Benites *et al.*, 1992).

For $0.12 < ka < 0.23$, the $1/Q_s$ is proportional to $(ka)^4$. This result is different from the one where $1/Q_s$ is proportional to f^2 based on the Rayleigh scattering criterion. When ka is small, the medium can be considered homogeneous with a lower density and a smaller velocity, thus leading to an increase in the scattering amplitude and a decrease in the scattering effect. The scattering medium used in the experiment is like the zone with cracks, fractures and/or pores in the crust. Accordingly, the relationship between $1/Q_s$ and ka obtained in this experiment can be employed for Q estimation in the crust, especially at low frequencies. With 2-D physical modelling, Matsunami (1979) investigated the scattering attenuation for long wave length approximation ($0.085 < ka < 0.58$). He found that the scattering attenuation coefficients for P- and S-waves were identical when they had the same ka values. Similarly, this study finds that the scattering attenuation coefficients still have the same results, even though the ka range is widened to $0.05 < ka < 10$.

6. CONCLUSIONS

On the basis of physical modelling experiments, the following conclusions of scattering effects can be made:

(1) For $ka \leq 0.05$, the scattering effect is very weak, and the medium can be considered homogeneous.

(2) The peak value of $1/Q_s$ appears at about ka = 0.5. For the high frequency, the $1/Q_s$ is proportional to $(ka)^{-1}$. For the low frequency, the curve of $1/Q_s$ versus ka is steeper than that predicated from Rayleigh scattering.

(3) For $0.05 < ka < 10.1$, the scattering attenuation coefficients for P- and S-waves are equal when they have the same ka values.

Acknowledgments The authors thank Dr. L. L. Tsai for improving the manuscript and Dr. K. F. Ma for providing valuable comments. Gratitude is also extended to the reviewers for their helpful comments. This study was supported by the National Science Council of the R.O.C. under Grant No. NSC81-0202-M008-02.

REFERENCES

Aki, K., 1980: Attenuation of shear waves in the lithosphere for frequencies from 0.05 to 25 Hz. *Phys. Earth Planet. Inter.*, **21**, 50-60.

Aki, K., and P. Richards, 1980: Quantitative Seismology I and II, Freeman and Co., San Francisco, p.932.

Benites, R., K. Aki, and K. Yomogida, 1992: Multiple scattering of SH waves in 2-D media with many cavities. *PAGEOPH*, **138**, 353-390.

Frankel, A., and R. W. Clayton, 1986: Finite difference simulations of seismic scattering: Implications for the propagation of short-period seismic waves in the crust and models of crust heterogeneity. *J. Geophys. Res.*, **91**, 6465-6489.

Kawahara, J., and T. Yamashita, 1992: Scattering of elastic waves by a fracture zone containing randomly distributed cracks. *PAGEOPH*, **139**, 121-144.

Kikuchi, M., 1981a: Dispersion and attenuation of elastic waves due to multiple scattering from inclusions. *Phys. Earth Planet. Inter.*, **25**, 159-162.

Kikuchi, M., 1981b: Dispersion and attenuation of elastic waves due to multiple scattering from cracks. *Phys. Earth Planet. Inter.*, **27**, 100-105.

Matsunami, K., 1979: Scattering of P waves in a two-dimensional model of a medium with random velocity fluctuation, Ann. Disaster Prevention Res. Inst., Kyoto Univ., 22-B: 91-105(in Japanese).

Matsunami, K., 1991: Laboratory tests of excitation and attenuation of coda waves using 2-D models of scattering media. *Phys. Earth Planet. Inter.*, **67**, 36-47.

Menke, W., 1984: Asymptotic formulas for the apparent Q of weakly scattering three-dimensional media. *Bull. Seism. Soc. Am.*, **74**, 1079-1081.

Menke, W., D. Witte, and R. Chen, 1985: Laboratory test of apparent attenuation formulas. *Bull. Seism. Soc. Am.*, **75**, 1383-1393.

Pant, D. R., S. A. Greenhalgh, and S. Waston, 1988: Seismic reflection scale model facility. *Explor. Geophys.*, **19**, 499-512.

Sato, H., 1982: Attenuation of S waves due to scattering by its random velocity structure. *J. Geophys. Res.*, **87**, 7779-7785.

Sato, H., 1984: Attenuation and envelope formation of three-component seismograms of small local earthquakes in randomly inhomogeneous lithosphere. *J. Geophys. Res.*, **89**, 1221-1241.

Wu, R. S., and K. Aki, 1988: Introduction: Seismic wave scattering in three dimensionally heterogeneous earth. *PAGEOPH*, **128**, 1-6.

Yamashita, T., 1990: Attenuation and dispersion of SH waves due to scattering by randomly distributed cracks. *PAGEOPH*, **132**, 545-568.